Fracture Toughness and Subcritical Crack Growth of Austenitic Manganese Steel

by R. I. Stephens,
Professor, Mech. Eng. Dept., U. of Iowa, Iowa City, Iowa, USA
C. P. Saxena
Research Asst., Mech. Eng. Dept. U. of Iowa, Iowa City, Iowa, USA
and R. C. Rice
Research Asst., Mech. Eng. Dept. U. of Iowa, Iowa City, Iowa, USA

Austenitic manganese (Hadfield) steel, due to its high strain hardening capacity has been used for almost 90 years in components which must withstand high repeated impact and wear conditions. Little is known about its quantitative cyclic stress-strain behavior, fracture toughness and fatigue crack growth behavior. The objective of this paper is to provide this quantitative behavior for two plate thicknesses from two different heats. Plate stock, 1/4 in. and 1 in. thick, was obtained by hot rolling at 1920°F followed by a water quench. The chemical composition varied in the two heats and is given in Table 1 as percentage by weight. It was not possible to obtain the two thicknesses from the same heat.

CYCLIC STRAIN HARDENING: Monotonic tensile and cyclic stress-strain behavior for 1/4 in. stock is shown in Fig. 1. Mechanical properties for both thicknesses, which varied somewhat, are given in Table 1 where: S_y = .2% yield strength in ksi., S_u = ultimate strength in ksi., σ_F = true fracture stress in ksi., m = monotonic strain hardening exponent at large strains, R_c = Rockwell hardness and K_c = plane stress fracture toughness in ksi$\sqrt{\text{in.}}$. Two strain scales are used in Fig. 1 to emphasize the cyclic strain hardening behavior of Hadfield steel. Solid dots on the cyclic stress-strain curve in Fig. 1 were obtained from the tips of steady-state hysteresis loops shown in Fig. 2. These hysteresis loops were obtained at 0.1 Hz frequency under constant axial strain amplitude incremental

testing.(1) It is evident that Hadfield steel cyclically strain hardens. Cyclic strain hardening was also obtained after 10% tensile overstrain during constant strain amplitude fatigue testing.(2)

FRACTURE TOUGHNESS: Fracture toughness and fatigue crack propagation for both thicknesses were obtained using pin loaded 4 in. x 3.94 in. compact tension specimens.(3) Tests were carried out on a MTS closed-loop electrohydraulic test system. Precracking was done under cyclic loading with ΔK less than 35 ksi$\sqrt{in.}$ A Chevron starter notch was used in some tests and a flat starter notch was used in others. Precrack lengths were 1.6 in. for fracture toughness testing and 1.0 in. for the fatigue crack growth study. Typical load crack opening displacement obtained under load control is shown in Fig. 3. Appreciable crack opening and plasticity with no pop-in occurred in all tests before fracture. Two specimens were tested for each thickness and average values of K_c given in Table 1 were 135 ksi$\sqrt{in.}$ and 150 ksi$\sqrt{in.}$ respectively for the 1/4 in. and 1 in. plate. K_c was calculated from $K_c = C_3 P/B\sqrt{W}$ (3), where: C_3 is the compliance constant, P is the load at crack instability, B is the specimen thickness and W was 3.2 inches. Valid K_{Ic} values were not obtained due to low yield strengths and large ductility. Fracture surfaces are shown in Fig. 4 and despite appreciable flat fracture with just slight shear lip formation, appreciable necking occurred in both thicknesses. Despite the greater thickness, the 1 in. plate had a higher fracture toughness than the 1/4 in. thickness. This is consistent however with the greater ductility of the 1 in. material.

FATIGUE CRACK GROWTH: Fatigue crack growth behavior was obtained at 15-20 Hz with $R = K_{min}/K_{max} = .01$. Mill scale was ground off in the crack region to a depth of about 0.005 in. on each side to

facilitate proper crack monitoring and to remove the undesirable decarberized martensitic surface skin. Specimens were loaded in the rolled direction. Crack growth was measured optically at 10X magnification with a traveling microscope and stroboscopic lighting. The least scale division was .001 in. Crack length versus applied cycles for the 1/4 in. material is shown in Fig. 5 for five different load ranges as indicated. Figures 6 and 7 show the crack growth rate versus stress intensity range for 1/4 in. and 1 in. material respectively. The data agrees well with the crack growth rate law proposed by Paris(4), $da/dN = A(\Delta K)^n$. Scatter band limits and mean values are indicated in Figures 6 and 7. For 1/4 in. material, A was $.2 \times 10^{-8}$ in./cycle and n was 2.39 while for 1 in. material, A was $.36 \times 10^{-8}$ in./cycle and n was 2.30. These values are comparable to those obtained by Barsom for many steels.(5)

Typical fatigue fracture surfaces for both thicknesses are shown in Fig. 8. Fatigue cracks propagated under flat plane strain conditions until final fracture at which appreciable necking is noted. Fig. 9 is a scanning electron fractograph for the 1/4 in. material showing fatigue striations. The surfaces were observed at a 45^o angle and only a small percentage of the actual fatigue crack growth surface contained striation markings.

REFERENCES

1. D. T. Raske and J. Morrow, Manual on Low Cycle Fatigue Testing, ASTM STP 465, 1969.
2. R. C. Rice and R. I. Stephens, Sixth National Symposium on Fracture Mechanics, Philadelphia, Pa. Aug., 1972.
3. ASTM, Tentative Method of Test, E399-70T.
4. P. C. Paris and F. Erdogan, J. of Basic Engineering, Dec., 1963.
5. J. M. Barsom, Damage Tolerance in Aircraft Structures, ASTM STP 486, 1971.

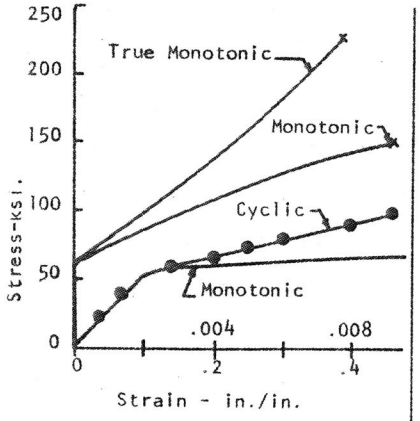

Fig. 1 Monotonic and Cyclic Stress-Strain Behavior (1/4 in.)

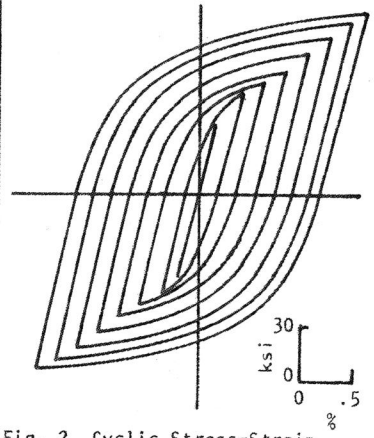

Fig. 2 Cyclic Stress-Strain Hysteresis Loops (1/4 in.)

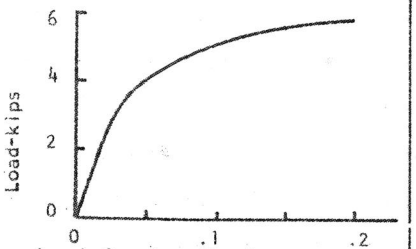

Fig. 3 Determination of Fracture Toughness (1/4 in.)

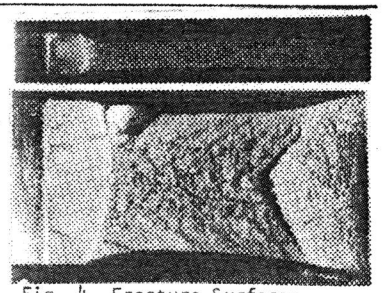

Fig. 4 Fracture Surfaces

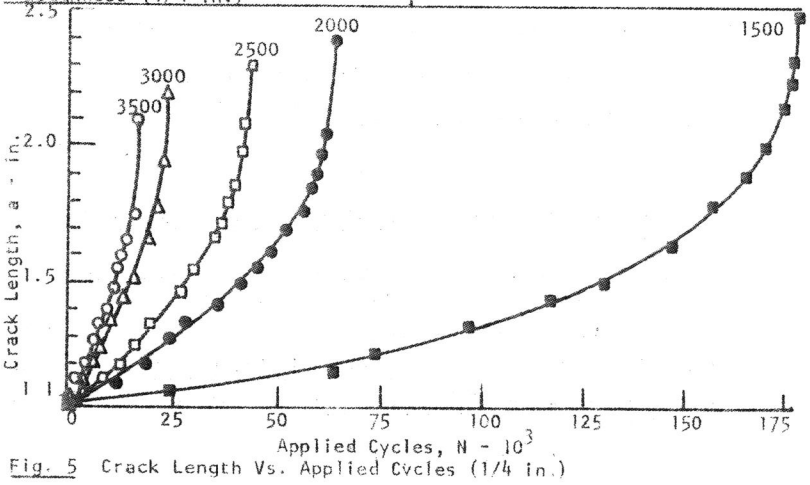

Fig. 5 Crack Length Vs. Applied Cycles (1/4 in.)

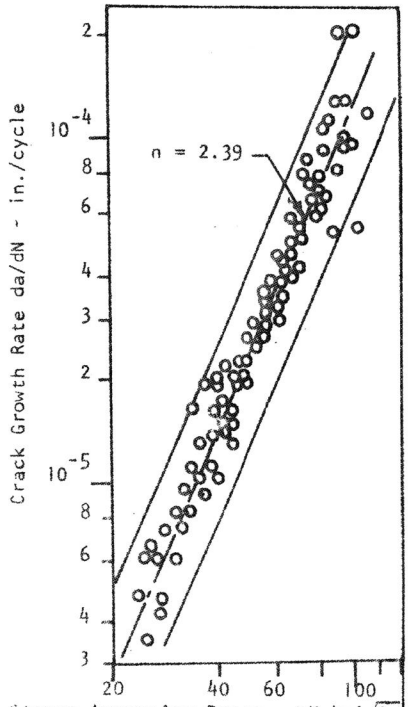

Fig. 6 Crack Growth Rate Vs. ΔK (1/4 in.)

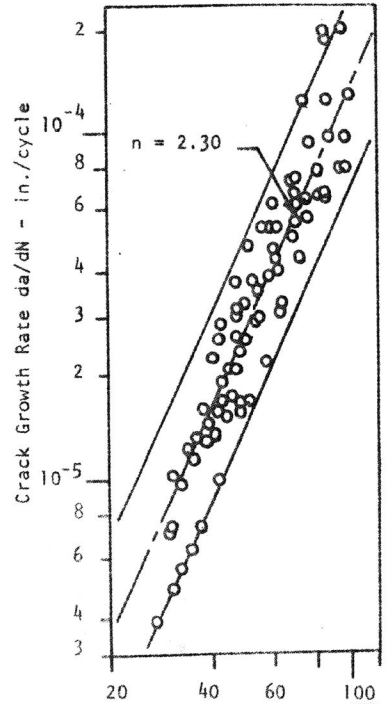

Fig. 7 Crack Growth Rate Vs. ΔK (1 in.)

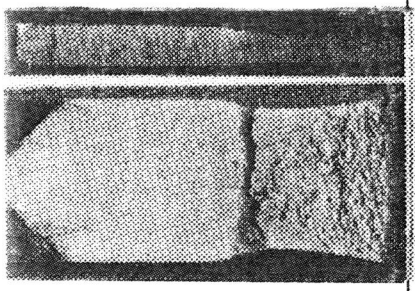

Fig. 8 Fracture Surfaces of Fatigue Crack Growth Specimens

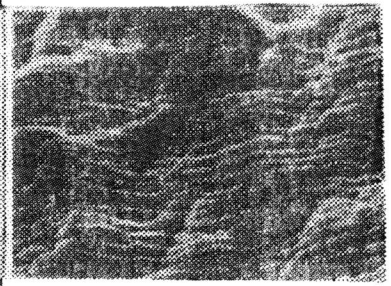

Fig. 9 Scanning Electron Fractograph 5700X (1/4 in.)

Table 1 Chemical Composition and Mechanical Properties

	C	Mn	P	S	Si	S_y	S_u	σ_f	%El.	%R.A.	m	R_c	K_c
1/4	1.1	12.5	.028	.009	.24	60	150	225	47	33	.7	23	135
1	1.21	12.7	.018	.009	.20	58	155	265	62	42	.6	23	150